DRF #137-0010
MAR 84-05
MLH01.DA

ANALYSIS OF THE VENT HEADER CRACKING AT HATCH 2

March 1984

Prepared by: _____
M. L. Herrera, Engineer
Mechanics Analysis

_____
K. R. Obermiller, Engineer
Mechanics Analysis

Approved by: _____
S. Ranganath, Manager
Mechanics Analysis

GENERAL ELECTRIC

TABLE OF CONTENTS

1. INTRODUCTION

Examination of the Hatch 2 vent header revealed a through-wall flaw which was nearly 360° of the header circumference in length. Figure 1 shows the vent header, and Figure 2 shows a sketch of the flaw. Metallurgical examination at General Electric Company of samples removed from the pipe containing the crack faces revealed that failure was in a brittle manner, and that crack initiation occurred near the butt weld at top center of the header. The most likely cause for brittle fracture is that the temperature of the vent header material, SA516 Gr. 70 carbon steel, dropped below the Nil Ductility Temperature (NDT). Below NDT, a material is susceptible to brittle fracture given that an initiated flaw and a driving force for crack propagation are present. Examination of the torus area in the vicinity of the failure showed that a nitrogen line was directly above the initiation location. Further investigation of the nitrogen injection system showed that cold nitrogen was deposited on the vent header on several occasions. The temperature of the nitrogen was capable of dropping the material temperature well below the NDT, and producing thermal stress that could cause crack extension.

Although the presence of the cracked vent header does not impede normal operation of the plant, depressurization during a Loss of Coolant Accident (LOCA) could be hampered by leakage of steam through the cracked area.

This analysis is for the purpose of addressing three key areas:

1. Determination of thermal stresses produced by cold nitrogen injection and if the observed cracking can be explained.

2. Determination that existing cracks, if any, grow through-wall and thus become detectable by leak monitoring.

3. Determination of maximum through-wall crack length that could be tolerated without pipe rupture during a LOCA event.

Responses to the above areas are required to explain the fracture of the vent header and to evaluate the consequence of an existing crack during a LOCA event.

2. THERMAL STRESS ANALYSIS

Method

Due to the complex three dimensional geometry of the structure, and applied thermal loading, the finite element method was used to determine the thermal stresses. The ANSYS computer program was used to perform the analysis. The three dimensional shell element (STIF 63) of the ANSYS element library was selected to model the vent header. This element is capable of both membrane and bending type stresses. Figure 3 shows the finite element model developed for the analysis. Due to symmetry about the butt weld, at which initiation is thought to have occurred, only half of the pipe, symmetric about the butt weld centerline, is required. The stiffener plate which lies on the bottom side of the pipe is simulated by increasing the thickness of the shell elements from .25 to .88 inch. The diameter of the pipe is 54 inches. The elements which comprise the stiffener plate are enclosed by the bold line in Figure 3. Appropriate boundary conditions at each end of the model were selected to simulate symmetry at one end and a long pipe at the other.

Material properties for SA516 Gr. 70 CS were used for the analysis.

Thermal Loading

The selection of temperature boundary conditions is a very crucial step in the analysis to accurately determine resulting stresses. The temperature distribution due to the injection of the nitrogen is not accurately known. Therefore, a temperature distribution will be assumed.

From Reference 1 impingement of a jet on a surface will cause a temperature distribution on the impacted surface in the shape of a Gaussian distribution (Figure 4). This shows that there will be a zone where the temperature of the surface can reach temperatures nearly equal to the jet fluid temperature.

Temperatures then drop off from the peak temperature and eventually reach ambient temperature. To simulate this behavior in the vent header finite element model, the temperature distribution shown in Figure 3 was used. The ambient temperature was assumed to be 100°F, while the nitrogen temperature was assumed to be -200°F.

The circumferentially cooled area was assumed to be from -90° to +90° from top dead center as illustrated. From -45° to +45° the temperature was assumed to be -200°F.

The assumed temperature distribution was incorporated into the model by assigning each individual shell element a temperature.

It is expected that a gross bending situation will occur due to the top of the header being cold and the bottom of the header being warm. The stiffener plates result in a wall thickness of over three times that of the .25 inch header pipe wall. This should result in bending of the cooled region inward and very little displacement and stress in the stiffened area.

Stress Analysis Results

As expected, the thermal cycling on the vent header causes large deflections at the top center location (approximately .1 inch). Figure 5 shows the displacement of the end nodal points which represent the center of the circumferential butt weld. The stiffener plates do not deflect as shown in the figure. The driving force for circumferential crack extension as experienced in the vent header is the applied axial stress. Crack extension requires a gross bending effect, which will produce tensile stresses in the upper portion of the vent header. The axial stress as obtained from the ANSYS computer output is shown in Figure 6 for the section of elements nearest the butt weld. Consistent with the displacement results, there is negligible stress in the stiffener plates. The influence of thickness and temperature discontinuity can be seen in the figure by the large tensile stress of approximately 19 ksi in the .25 inch material. The stress decreases to approximately 15 ksi in the area of crack initiation. The variation

circumferentially indicates that the stress at the crack initiation location could range anywhere from 15 ksi to 19 ksi depending on the cooled area location with respect to crack initiation location. If the cooled area center is not located near the crack initiation location (i.e., crack initiation location is on the edge of the cooled area), the stress could be higher than 15 ksi. For purposes of this analysis, a value of 15 ksi is used for the thermal stress. Two additional sources of stress in the vent header are cold spring stress and weld residual shrinkage stress due to welding of the support plates on the bottom half of the vent header. A cold spring stress of 15 ksi was used for the analysis. This is justified by the observed crack opening and transverse displacement of the crack faces after fracture. Assuming a .1 inch transverse displacement over 20 feet gives approximately 15 ksi cold spring stress. The determination of weld shrinkage residual stress due to welding of the support plates on the bottom of the vent header requires sophisticated elastic-plastic analysis. In this analysis, the weld shrinkage stress was conservatively omitted.

The potential for crack growth is analyzed by the use of Linear Elastic Fracture Mechanics (LEFM) which assumed brittle behavior. This is consistent with the metallurgical finding.

The stress intensity factor is calculated by the use of the following equation from Reference 2,

$$K_I = \sigma_m M_m \sqrt{\pi a/Q} + \sigma_b M_b \sqrt{\pi a/Q}$$

where σ_m = membrane stress
σ_b = bending stress
M_m = membrane correction factor
M_b = bending correction factor
a = crack depth
Q = shape factor

The membrane stress is comprised of the cold spring stress and thermal stress. Weld residual stress comprises the bending stress component.

An initial flaw size of .1 inch in depth and 2 inches in length was assumed. This is consistent with metallurgical findings. This is reasonable since the initial shock stress, coupled with the residual stress, could easily drive smaller flaws to .1 inch in depth.

The membrane and bending correction factor, and the shape factor, are obtained from Reference 2.

$$M_m = 1.74$$
$$M_b = 1.00$$
$$Q = 0.84$$

The stress intensity factor for the assumed loads and crack depth is 56.4 $ksi\sqrt{in.}$

Impact testing of SA516 Gr. 70 samples removed from the Hatch vent header indicates an NDT of below -50°F. Charpy data taken from the impact testing is shown in Table 1. This data must be corrected due to sub-size specimens. With correction, impact energy values are as low as 8 ft-lbs.

Table 1

Temperature (°F)	Impact (ft-lbs)
40	12.5, 11.5, 11.0
20	11.5, 11.5, 11.0
0	11.5, 11.5, 12.0
-20	11.0, 11.0, 11.0
-40	11.0, 10.5, 11.5
-60	6.0, 9.0, 9.5
-80	4.0, 5.0, 8.0

From Reference 3, a correlation between Charpy hardness and fracture toughness is obtained. For low alloy steel the correlation is

$$\frac{K_{IC}^2}{E} = 5\ (CVN)$$

This gives

$$K_{IC} = 31.0 \text{ ksi}\sqrt{\text{in.}}$$

This fracture toughness corresponds to the plane strain condition. Since the vent header wall is only .25 inch thick, the plane stress condition is appropriate. The plane stress fracture toughness can be found by using Irwin's correction factor. The plane stress, stress intensity factor, is:

$$K_C^2 = K_{IC}^2[1 + 1.4\ \beta_{IC}^2]$$

where

$$\beta_{IC} = \frac{1}{t}\left(\frac{K_{IC}}{\sigma_{ys}}\right)^2$$

The correction factor is valid only for $0.4 \leq \beta_{IC} \leq 1.0$. Since β_{IC} is greater than 1 for this case, a value of 1 is assumed. This results in $K_c = 48$ ksi$\sqrt{\text{in.}}$

The applied stress intensity factor (56.4 ksi$\sqrt{\text{in.}}$) is above the material fracture toughness, indicating that the part-through crack will grow through the wall thickness and become a through-wall crack.

Once a through-wall crack has occurred, circumferential crack propagation could occur if applied loads are large enough. The driving force for circumferential crack extension is the thermal stress from nitrogen injection and cold spring stress which total to 30 ksi. From Reference 4 the stress intensity factor for a shell with a circumferential crack of length 2a is

$$K_I = C\sigma\sqrt{\pi a}$$

where $C \sim 1.1$

This results in a stress intensity factor of approximately 58 ksi$\sqrt{\text{in.}}$ This is above the material toughness of 48 ksi$\sqrt{\text{in.}}$ indicating that circumferential crack growth will occur once cracks have grown through-wall. The conclusions on brittle fracture are consistent with metallographic fracture evidence, suggesting a brittle fracture mechanism.

3. LIKELIHOOD OF THROUGH-WALL CRACKING

Since detection of cracking in the vent header piping is by visual examination or leak monitoring, it is necessary to know whether cold nitrogen insertion can cause large part-through cracks that may not be detected by the visual/leak tests. As shown in the earlier analysis on the evaluation of the Hatch 2 cracking, exposures to cold nitrogen cause high thermal shock stresses. This, coupled with the weld residual stresses, can cause crack initiation. The stress intensity factors for such cracks increases with crack depth. Therefore, once crack initiation occurs (starting from say, a weld defect), it will continue to propagate until the crack penetrates the backwall. At this point, circumferential crack extension will occur due to the gross section stresses such as thermal bending or cold spring stress. Crack arrest will occur when the crack tip ends up in higher toughness material that is not exposed to the cryogenic nitrogen.

Based on the above discussion it is concluded that exposure to cold nitrogen will lead to through-wall cracks which can be monitored by visual examination or leak testing.

4. CRITICAL CRACK SIZE FOR THE VENT HEADER DURING A LOCA EVENT

The purpose of this section of the report is to determine the maximum through-wall crack that can be sustained in the vent header without inducing crack propagation. This analysis is based on linear elastic fracture mechanics (LEFM) methods. The use of LEFM is conservative since the material will most likely exhibit ductile behavior during any crack propagation.

The two main loads that act on the vent header during a loss of coolant accident (LOCA) are the pressure differential and the pool swell impact loads. These loads are defined in Figure H2 4.1.1-1 and Table H2 4.3.3-1 of Reference 5. Other loads are present; however, they are transmitted directly to the vent header supports.

The most severe loads occur about .5 second after the initiation of the LOCA. At this time the pressure differential in the vent header is 24 psi. The axial membrane stress induced by this pressure is:

$$\sigma_m = \frac{pr}{2t} = \frac{(24\ \text{psi})(27\ \text{in.})}{2(.25\ \text{in.})} = 1.3\ \text{ksi}$$

When analyzing the effect of the pool swell impact loads, the 20 foot section of the vent header between supports is assumed to act like a uniformly loaded, simply supported beam. An average pressure of 11.18 psi is applied to the vent header which translates into a load of 604 lbs per inch. The maximum bending stress associated with this load is

$$\sigma_b = \frac{Mc}{I} = \frac{wl^2 c}{8I} = \frac{wl^2 R_o}{8\left(\pi/4(R_o^4 - R_i^4)\right)}$$

This gives a bending stress of 7.56 ksi. The maximum stress in the vent header due to these two loads is, therefore, 8.86 ksi. The applied stress intensity factor can be obtained from Reference 6.

$$K_I = F_p(\lambda)\ \sigma_t \sqrt{\pi a} + C(a)\ F_p(\lambda)\ \sigma_b \sqrt{\pi a}$$

where a = half crack length

$\lambda = a/\sqrt{Rt}$

$\gamma = a/\pi R$

$$F_p(\lambda) = (1 + 0.3225\ \lambda^2)^{1/2} \quad \text{for } 0 \leq \lambda \leq 1$$

$$= 0.9 + 0.25\ \lambda \quad \text{for } 1 < \lambda \leq 5$$

$$C(a) = \frac{1 + 6.8\ \gamma^{3/2} - 13.6\ \gamma^{5/2} + 20\ \gamma^{7/2}}{1 + 7.5\ \gamma^{3/2} - 15\ \gamma^{5/2} + 33\ \gamma^{7/2}}$$

Figure 7 shows K_I as a function of crack length.

Figure 8 shows the curve used to determine the plane strain fracture toughness, K_{IC}. This figure was taken from Reference 2. Although this curve

is specifically for low alloy steels, it also represents a conservative estimate of the fracture toughness for carbon steels. Figure M2 4.1.1-2 of Reference 5 specifies the temperature of the vent header to be 85°F at the beginning of a LOCA. If a conservative value of 0°F is assumed for the NDT reference temperature, the corresponding fracture toughness is 160 ksi$\sqrt{\text{in.}}$ Using Irwin's correction factor for plane stress behavior, the plane stress fracture toughness, K_C, can be obtained.

$$K_C^2 = K_{IC}^2 \left[1 + 1.4\ \beta_{IC}^2\right]$$

$$\text{where } \beta_{IC} = \frac{1}{t}\left(\frac{K_{IC}}{\sigma_{ys}}\right)^2$$

This equation is valid for $0.4 \leq \beta_{IC} \leq 1.0$. In the present cases B_{IC} is greater than one, so a value of one was used.

For $RT_{NDT} = 0°F$

$$K_C = \left[(160 \text{ ksi in.})^2(1 + 1.4)\right]^{1/2} = 248 \text{ ksi in.}$$

K_C will be conservatively taken to be 200 ksi$\sqrt{\text{in.}}$ since at such high levels of toughness the mode of failure is ductile rather than brittle.

Cracks which are long enough to result in applied stress intensity factors above these fracture toughness levels will propagate and cause failure. This limit is shown in Figure 7. The crack length corresponding to the assumed RT_{NDT} of 0°F is approximately 40 inches. If cracks exist in the vent header and are not detected by visual inspection or other means, they are most likely well below the critical crack length. Therefore, they will not inhibit the vent header from performing its required function during a LOCA.

5. CONCLUSION

The analysis presented here shows that the Hatch vent header cracking can be expected, given the liquid nitrogen injection and the applied loadings. The resulting cracks are expected to be through-wall so that they can be monitored by visual observation or leak tests. Finally, the critical crack length during a LOCA event is large enough that cracks would be detected by routine visual inspection or other examinations.

6. REFERENCES

1. Schlicting, H., 'Boundary Layer Theory,' Pergamon Press, New York, 1955.

2. ASME Boiler and Pressure Vessel Code, Section XI, 1983 Edition.

3. Rolfe, S., Barsom, J., 'Fracture and Fatigue Control in Structures,' Prentice-Hall, Inc., Englewood Cliffs, New Jersey, 1977.

4. Rooke, D., Cartwright, D., 'Stress Intensity Factors,' The Hillingdon Press, Uxbridge, Middlesex, England, 1976.

5. 'Mark I Containment Program Plant Unique Load Definition, Edwin I. Hatch Nuclear Plant—Unit 2,' September 1981, NEDO 24569 Rev. 2.

6. 'The Application of Fracture-Proof Design Methods Using Tearing Instability Theory to Nuclear Piping Postulating Circumferential Through Wall Cracks,' NUREG/CR-3464, Del Research Corporation, EG+G, Idaho, Inc.

MLH01.da

7. FIGURES

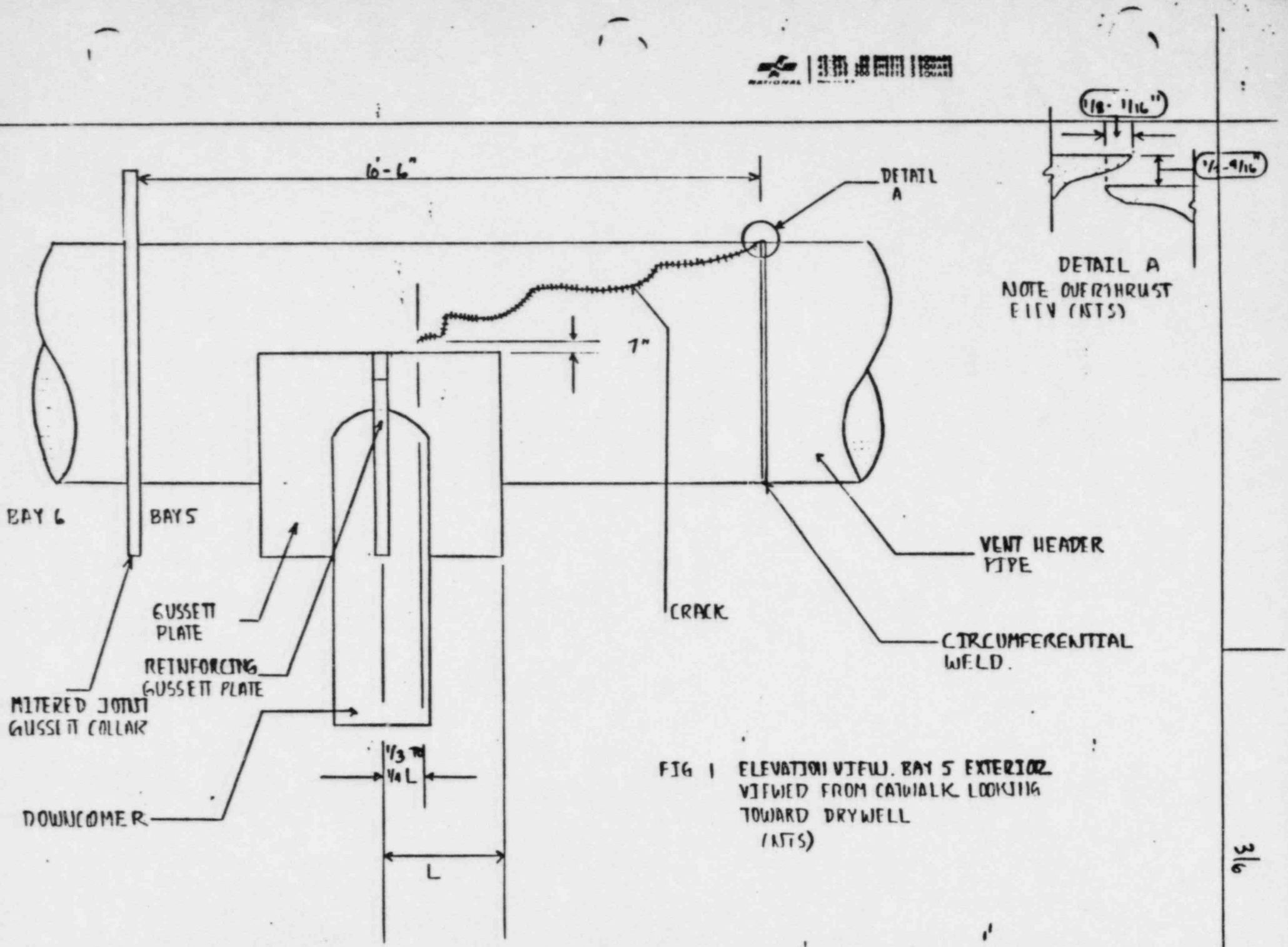

FIG 1 ELEVATION VIEW. BAY 5 EXTERIOR VIEWED FROM CATWALK LOOKING TOWARD DRYWELL (ATTS)

RFE
4-84
DM
4-84

14'-1 5/8" CIRC.

34" DIA

FIGURE 2. SCHEMATIC SHOWING FRACTURE

PRELIMINARY AS-FOUND SKETCH
VIEW OF PIPE CUT & UNROLLED

SCALE: 3/4" = 1'-0" REV A

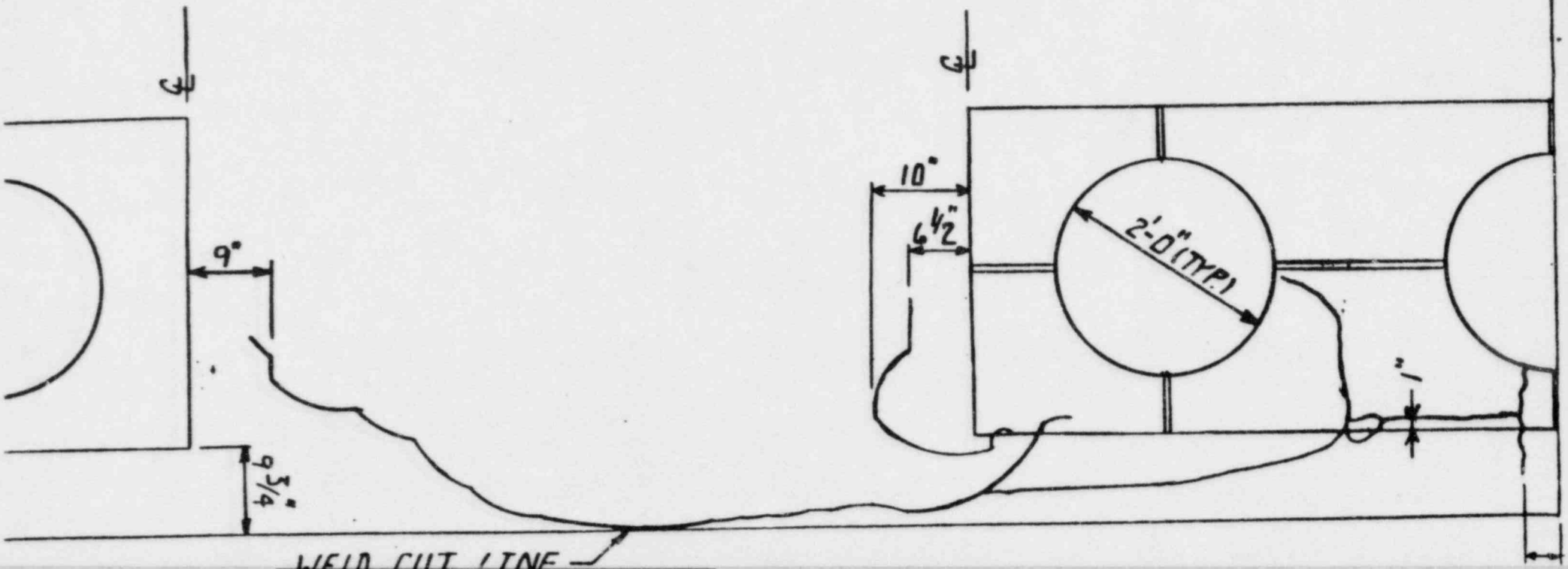

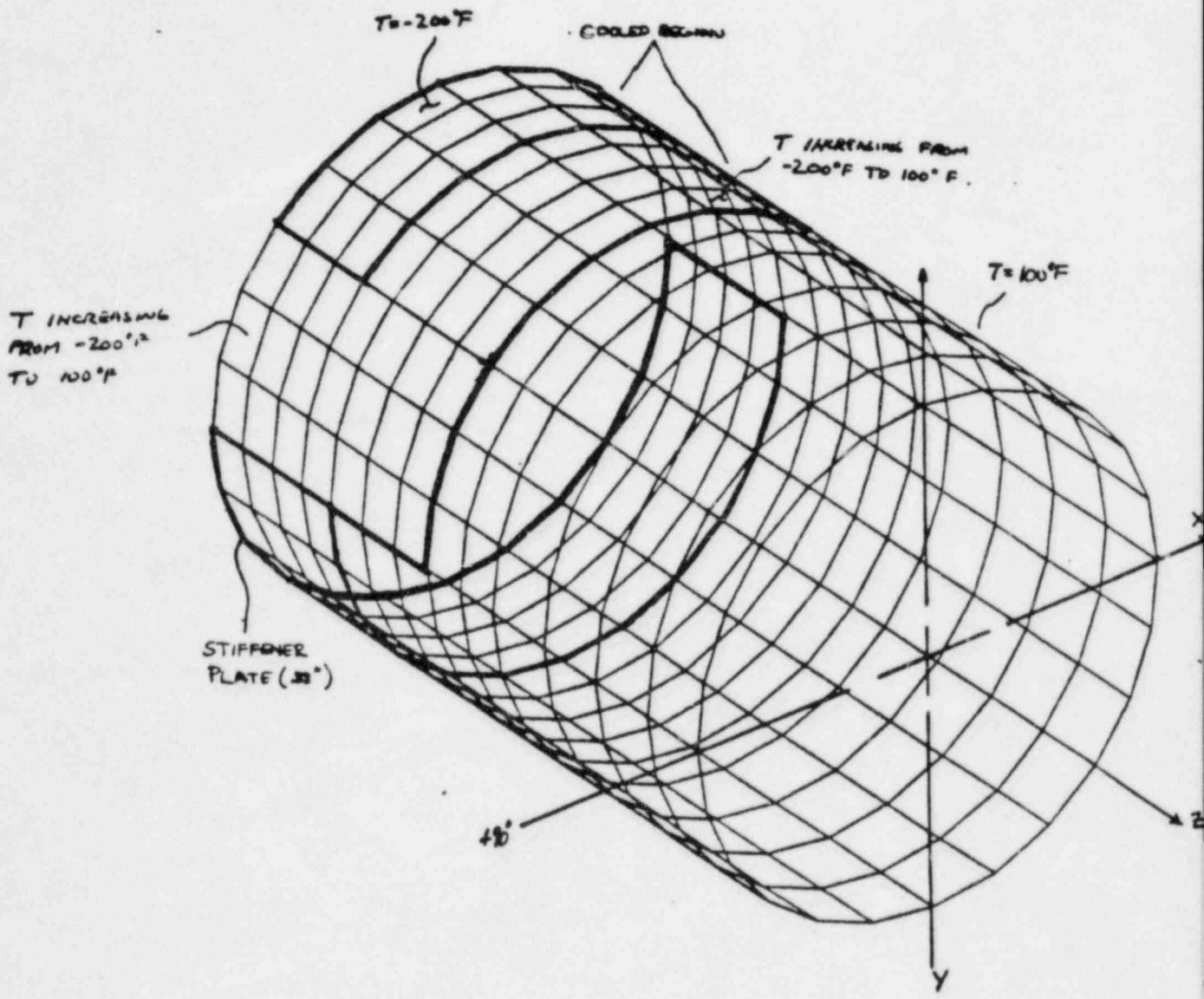

FIGURE 3. FINITE ELEMENT MODEL OF VENT HEADER

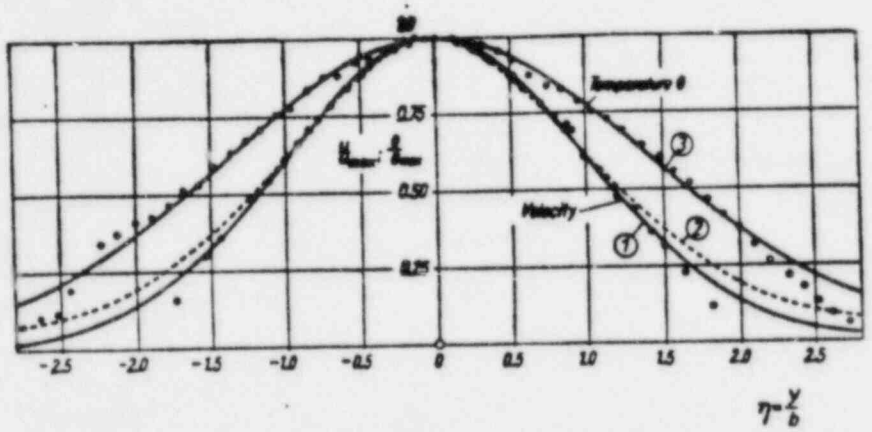

Fig. 4 Temperature and velocity distribution in a two-dimensional jet. Measurements are due to Reichardt [4]. Curve (1): $u/u_{max} = \exp(-\frac{1}{2}\eta^2)$; curve (2): $u/u_{max} = 1 - \tanh^2(K\eta)$, eqn. (22.45); curve (3): $\vartheta/\vartheta_{max} = \exp(-\frac{1}{2}\eta^2) = (u/u_{max})^{1/n}$

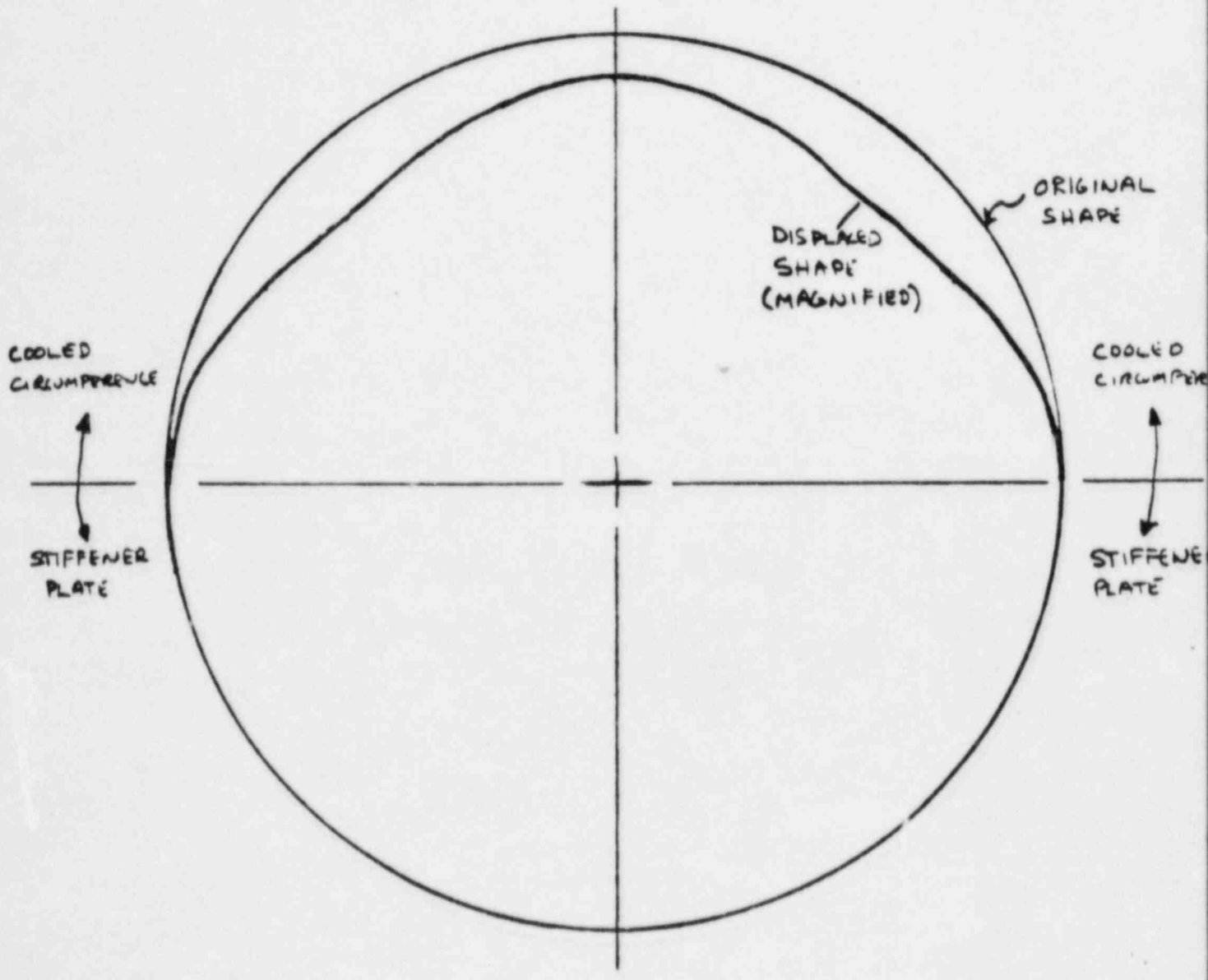

FIGURE 5 - DISPLACEMENTS AT BOTT-WELD CENTERLINE

(NOT TO SCALE)

FIGURE (6) STRESS AT BUTT WELD CIRCUMFERENTIAL POSITION

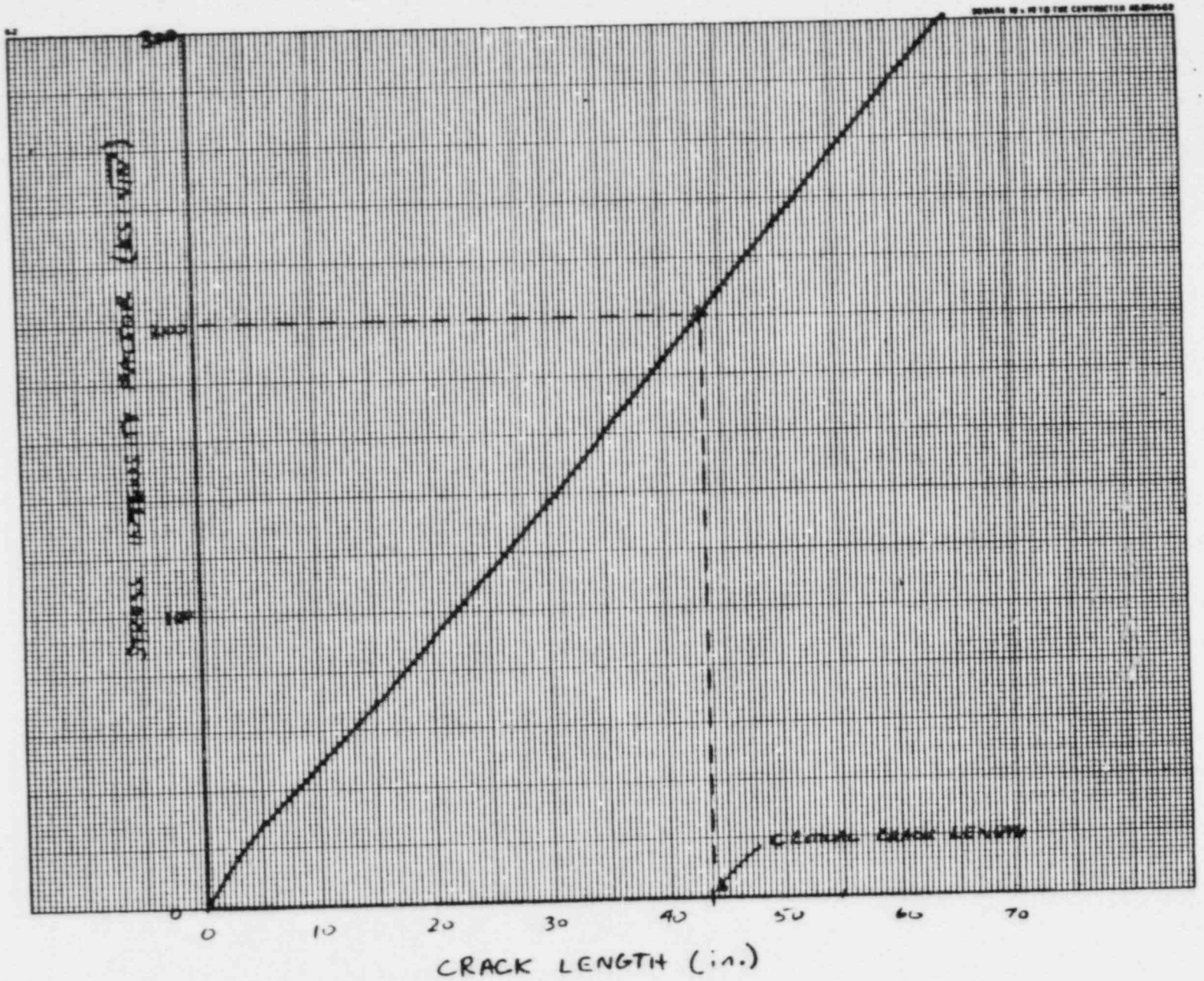

FIGURE 7 - STRESS INTENSITY VERSUS CRACK LENGTH

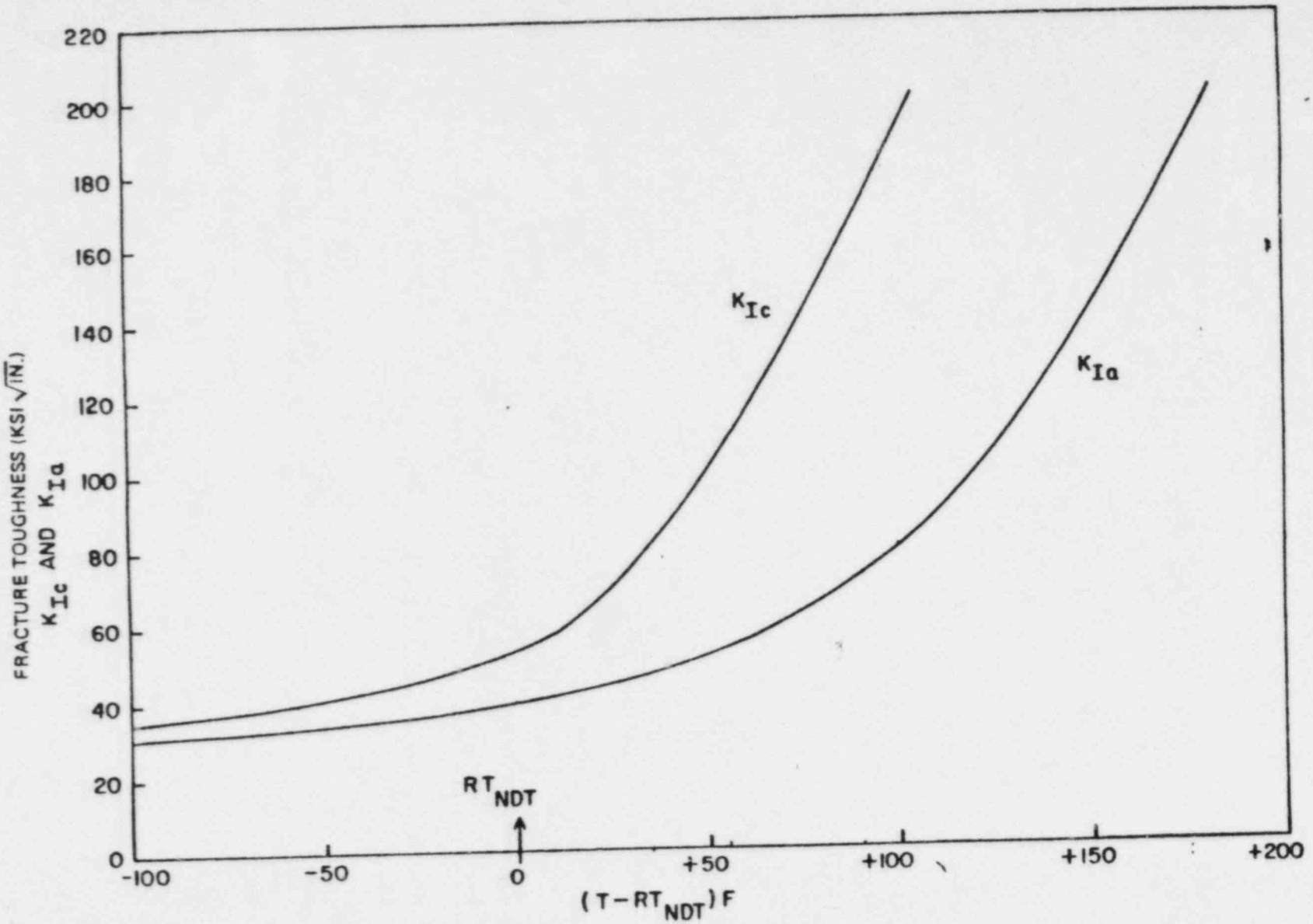

FIG 8. FRACTURE TOUGHNESS FOR LOW ALLOY STEEL